Hydrogen absorption by Zr–1Nb alloy with TiN$_x$ film deposited by filtered cathodic vacuum arc

E B Kashkarov[1], N N Nikitenkov[1], M S Syrtanov[1] and M N Babihina[1]

[1]Tomsk Polytechnic University, 30 Lenin Avenue, Tomsk, Russian Federation

E-mail: egor_kashkarov@mail.ru

Abstract. This paper describes the opportunity of titanium nitride (TiN$_x$) films application as protective coating for Zr-2.5Nb alloy from hydrogenation. Dense TiN$_x$ films were prepared by filtered cathodic vacuum arc (CVA). Hydrogen absorption rate was calculated from the kinetic curves of hydrogen sorption at elevated temperature of the sample (T = 673 K) and pressure (P = 2 atm). Results revealed that TiN$_x$ films significantly reduced hydrogen absorption rate of Zr-2.5Nb.

1. Introduction

Zirconium-based alloys such as Zr–1Nb, Zr–2.5Nb are widely used in nuclear industry as cladding materials for Russian PWR of VVER type reactors. Zirconium has a good combination of properties such as low neutron absorption, stress-corrosion cracking resistance, creep behavior, reduced hydrogen uptake and corrosion [1–3]. Hydrogen released during the process of water radiolysis which appeared under the influence of radiation during reactor operation cycle. Hydrogen degradation can manifest itself in appearance of hydride phases resulting in substantial loss of plasticity, increase in ductile-brittle transition and sometimes in decrease in mechanical strength [4-9]. The presence of high temperatures, pressure, mechanical loads lead to the mechanical properties degradation [5-10].

Most attempts to prevent hydrogen embrittlement of zirconium alloys focused on the surface modification and deposition of thin surface layers by ion-plasma deposition, ion implantation, pulsed electron or ion beams surface modification [11-13]. TiN$_x$ is a promising candidate as a diffusion barrier coating. It has high melting temperature, high hardness, excellent exhibited ion-irradiation tolerance and high thermal conductivity [14–17]. TiN thin films have found a numerous industrial application because high erosion and corrosion resistance which favorably affects the fretting wear of the coating [18]. It was previously found that TiN$_x$ films deposited by direct current magnetron sputtering (dcMS) significantly reduced hydrogen uptake by Zr–1Nb alloy and it is promising films to protect zirconium alloys from hydrogen embrittlement [19, 20]. However, the sputtered TiN films usually exhibits a lower density and adhesion with substrate compared to arc evaporated films due to its low density and degree of ionized sputtered atoms. Additionally, magnetron sputtering always exhibits lower deposition rate due to target poisoning with an introduction of reactive gas. Cathodic vacuum arc (CVA) deposition has some advantages such as a high ion to neutral ratio of arc evaporation process which resulted in a densification of the growing film and a high level of adhesion to the substrate due to increased adatom mobility [21]. The formation of macro-particles during arc evaporation leads to a defect and rough surface morphology of coating [22, 23]. It was demonstrated that the application of plasma filters and negative pulsed bias to a substrate significantly reduced the microdroplets content in coatings [24, 25].

Hydrogen absorption kinetics by Zr–1Nb alloy with TiN$_x$ films deposited by filtered CVA have not been discussed. In this paper we described the influence of TiN$_x$ deposited by filtered CVA onto Zr–1Nb alloy on hydrogen absorption rate and element distribution before and after hydrogen saturation.

2. Materials and Methods

Zr–1Nb samples with fixed size of 20×20×0.5 mm were previously polished to the average roughness R$_a$ of 0.045 μm using sandpaper and diamond paste. The chamber was evacuated to the base pressure of lower than 2.5×10^{-3} Pa. Before deposition samples were subjected to ion bombardment in argon glow

discharge at 1500 V for 3 min. The cathodic vacuum arc evaporation system equipped with coaxial plasma filter (designed by authors [2**4**]) was used. Ti (99.99 % purity) was used as the cathode material. The process parameters are shown in Table 1.

Table 1. Process parameters for TiN_x coatings deposition

Arc current, A	Pulsed bias, V	Pulse frequency, kHz	Pressure (Ar), Pa	Deposition time, min
75	150	100	0.15	30

Hydrogenation of the samples was performed by Sievert method (from hydrogen atmosphere) on the automated complex Gas Reaction Controller LPB (USA) during 120 min at 673 K temperature. The heating rate and hydrogen pressure in the chamber was 6 K/min and 2 atm respectively. The hydrogenation temperature was chosen due to the working temperature of zirconium fuel cladding in the operation process of nuclear reactors. Hydrogen absorption rate was measured from the absorption curves after hydrogen saturation.

The phase identification and structural investigations were performed by X-ray diffraction with CuKα radiation (1.5410 A wavelength) using Shimadzu XRD-7000 (Japan) diffractometer in asymmetric mode at 40 kV, 30 mA and θ=3° fixed angle. Study of the elemental composition of samples was performed by high-frequency glow discharge optical emission spectroscopy (GD-OES) with GD-Profiler 2 technique (Horiba, Japan). Hydrogen concentration was measured according to the principle of melting in inert gas at hydrogen analyzer RHEN602 (LECO, USA).

3. Results and discussion

Figure 1 shows that the intensity of hydrogen pick-up by Zr–1Nb significantly higher than Zr–1Nb with TiN_x. Hydrogenation of initial zirconium alloy characterized by a linear region at the beginning of the process and gradually reaches saturation to 2500 sec in comparison with $Zr–1Nb/TiN_x$ which has not reached saturation during hydrogenation. Thus, TiN_x film deposited by filtered CVA reduces the intensity of hydrogen uptake by Zr–1Nb alloy. The average hydrogen absorption rate was calculated on the linear
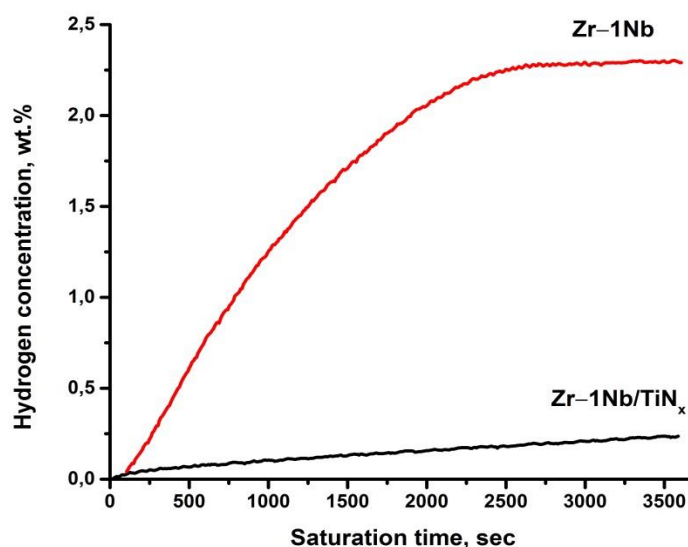

Figure 1. Hydrogen pick-up curve

regions and presented in Table 2. Hydrogen absorption rate by Zr–1Nb decreased in ~24 times as a result of TiN_x coating deposition.

Table 2. Average hydrogen absorption rate

Sample	Average hydrogen absorption rate, wt.%/sec
Zr–1Nb	1.4×10^{-3}
$Zr–1Nb/TiN_x$	5.7×10^{-5}

Table 3 shows that after hydrogen saturation the total hydrogen concentration in the volume decreased from 22100±300 ppm for Zr–1Nb to 1150±100 ppm for Zr–1Nb with TiN_x film. The principle of melting in inert gas at hydrogen analyzer allows to measure hydrogen concentration with the accuracy of less than 1 ppm. However, the concentration of hydrogen is generally distributed unevenly throughout the sample volume. Therefore we cut 3 pieces from different sites of the samples to more accurately determine the

total hydrogen concentration. The small amount of hydrogen contained in initial Zr–1Nb and Zr–1Nb/TiN$_x$ samples.

Table 3. Hydrogen concentration in the samples before and after hydrogen saturation

Hydrogen concentration	Zr–1Nb	Zr–1Nb/TiN$_x$
Before saturation	14±3 ppm	19±5 ppm
After saturation	22100±300 ppm	1150±100

Figure 3 shows diffraction patterns of Zr–1Nb with TiN$_x$ coating before and after hydrogen saturation. In-plane XRD measurements were carried out in an asymmetrical layout. The incidence angle was 3 degree. The zirconium hydride reflections have been observed after hydrogenation. Analysis of this pattern shows that zirconium hydride reflections belong to the δ hydride. The most intensive reflection (200) of TiN coatings has been detected in both diffraction patterns. This fact indicates on the presence of the texture in the coatings. It could be associated with TiN$_x$ coatings deposition parameters.
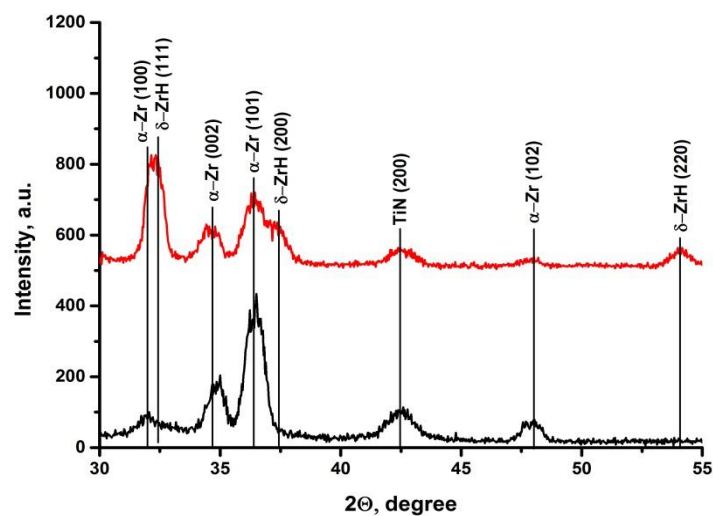

Figure 3. XRD analysis of Zr–1Nb with TiN$_x$ before (below) and after (above) hydrogenation

Figure 4 shows GDOES profiles of Zr, Ti, N, O, H elements before and after hydrogen saturation. The results revealed that hydrogen is present in the TiN$_x$ film and non-uniformly distributed in the sample volume after hydrogen saturation. Furthermore the thin oxide film was observed on the surface of the samples before and after hydrogenation. The intensity of hydrogen signal monotonically decreased with increasing the analyzing depth (sputtering time) and nearly reaches the minimum behind the TiN$_x$–Zr–1Nb interface (Fig. 4a). It also can be seen that Ti/N ratio decreased at the film depth. After hydrogen
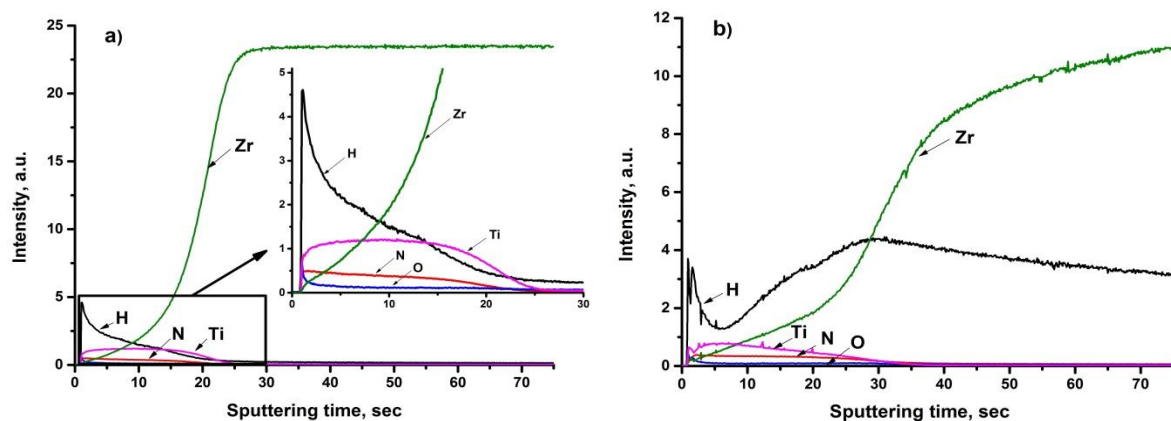

Figure 4. GDOES profiles of elements of Zr–1Nb/TiN$_x$ before (a) and after (b) hydrogen saturation

saturation the intensity of hydrogen signal increased and reached the maximum in TiN$_x$–Zr–1Nb interface than monotonically decreased with increasing the depth (Fig. 4b). It indicates that hydrogen accumulates

in the TiN$_x$ film towards the interface which is probably associated with the decreasing of nitrogen content. Hydrogen penetrates outside the TiN$_x$ film through Zr–1Nb alloy due to diffusion process induced by the difference of concentration in the interface and the sample volume.

4. Conclusion
Titanium nitride films deposited by filtered cathodic vacuum arc significantly reduced hydrogen uptake and total amount of hydrogen in the volume of Zr–1Nb alloy. Hydrogen absorption rate decreased in more than 20 times. δ-phase zirconium hydride formed during hydrogen saturation of Zr–1Nb with TiN$_x$ film. Hydrogen predominantly accumulates in the TiN$_x$–Zr–1Nb interface where the nitrogen content is low.

References
[1] Sabol G P 2004 Proc. 14th Intern. Symp. 3
[2] Murty K L 2006 Prog. Nucl. Energy **48** 325
[3] Montgomery R, Waeckel N, Yang R 2001 Proc. 29th Annual NRC Water Reactor Safety Meeting 409
[4] Chernyaeva T P, Ostapov A V 2013 *Voprosy atomnoy nauki i tehniki* **87** 16
[5] Silva K R, Dos Santos D S, Robeiro A F, Almeida L H 2010 *Defect and Diffusion Forum* **722** 297
[6] Zielinski A, Sobieszczyk S 2011 *Intern. Journ. of Hydrogen Energy* **36** 8619
[7] Bai J B 1993 *Scripta Metallurgica et Materialia* **29** 1259
[8] Mani Krishna K V, Sain A, Samajdar I, Dey G K 2006 *Acta Materialia* **54** 4665
[9] Singh R N, Kishore R, Singh S S, Sinha T K, Kashyap B P 2004 *Journ. of Nuclear Materials* **25** 26
[10] Anders A 2007 *Jour. Phys. D: Appl. Phys.* **40** 2272
[11] Lider A M, Chernov I P, Cherdantsev Yu P, Pushilina N S, Stepanova O M, Garanin G V 2010 *Proc. 16-th Symp. on High Current Electronics* **2** 541
[12] Ivanova S V, Glagovskiy E M, Khazov I A, Orlov V K, Shlepov I A, Nikitin K N, Dubrovskiy Yu V, Denisov E A 2008 *Proc. IV Int. Conf. on Interaction of Hydrogen Isotopes with Structural Materials* 51
[13] Nikitenkov N N, Sutygina A N, Shulepov I A , Sivin D O , Kashkarov E B 2015 *IOP Conf. Series: Materials Science and Engineering* **81** 012018
[14] Wang H, Araujo R, Swadener J G, Wang Y Q, Zhang X, Fu E G, Cagin T 2007 *Nucl. Instrum. Methods B* **261** 1162.
[15] Oyama S T 1996 *Chemistry of Transition Metal Carbides and Nitrides* (Berlin: Springer)
[16] Toth L E 1971 *Transition metal carbides and nitrides* (Academic Press)
[17] Pierson H O 1996 *Handbook of Refractory Carbides and Nitrides: Properties, Characteristics, Processing and Applications* (Noyes Publications)
[18] Hultman L 2000 *Vacuum* **57** 1
[19] Nikitenkov N N, Kashkarov E B, Tyurin Yu I, Nikiforova N I 2014 Izvestiya vuzov. Physika **57** (11/2) 134
[20] Kashkarov E B, Nikitenkov N N, Tyurin Yu I, Syrtanov M S, Zhang Le 2015 *Iop Conf. Series: Materials Science and Engeneering* **81** 012017
[21] Boxman R L, Martin P J, Sanders D M 1995 *Handbook of Vacuum Arc Science and Technology: Fundamentals and Applications* (NJ: Noyes) 367
[22] Karpov D A 1997 *Surf. Coat. Technol.* **96** (1997) 22
[23] Coll B F, Sanders D M 1996 *Surf. Coat. Technol.* **81** 42
[24] A.I. Ryabchikov, D.O. Sivin, A.I. Bumagina 2014 *Applied Surface Science* **310** 130
[25] Ryabchikov A I, Ryabchikov I A, Stepanov I B 2005 *Vacuum* **78** 331